

In Situ Neutron Scattering Study of the Structure Dynamics of the Ru/Ca₂N:e⁻ Catalyst in Ammonia Synthesis

Xinbin Yu,¹ Jisue Moon,¹ Yongqiang Cheng, Luke Daemen, Jue Liu, Sung Wng Kim, Abinash Kumar, Miaofang Chi, Victor Fung,* Anibal J. Ramirez-Cuesta, and Zili Wu*



Cite This: <https://doi.org/10.1021/acs.chemmater.2c03599>



Read Online

ACCESS |



Metrics & More

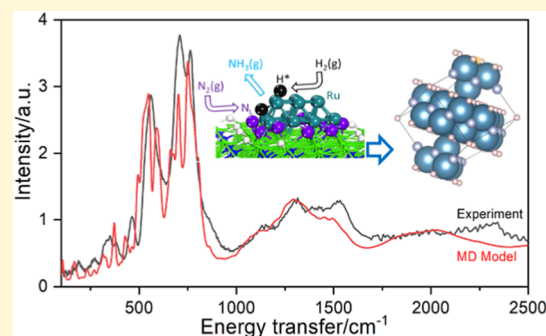


Article Recommendations



Supporting Information

ABSTRACT: NH₃ synthesis is one of the most critical industrial processes. Compared to commercial iron catalysts, Ru catalysts show high intrinsic activity in this reaction but suffer from hydrogen poisoning. By loading Ru onto supports such as electrides and hydrides, the hydrogen poisoning problem can be significantly alleviated. However, relevant studies on the structural dynamics of the Ru/electride catalysts under reaction conditions are very scarce. Taking advantage of the high sensitivity to hydrogen species, it is possible to obtain insights into the structural changes during the reaction using in situ neutron techniques. In this study, we have investigated the structural evolution of the Ru/Ca₂N:e⁻ catalyst during the ammonia synthesis reaction by in situ neutron scattering (inelastic neutron scattering, INS) technique. In situ INS experiments suggest that Ca₂N:e⁻ is likely converted to the Ca₂NH phase during the reaction. Unlike the previously known structure where H and N atoms are intermixed, the formed Ca₂NH exhibits a segregated structure where the H and N atoms are located in different layers separated by the Ca layer. Density functional theory calculations of the reaction energetics reveal that there are minor changes in the barriers and thermodynamics of the first N hydrogenation step between the two phases (Ca₂NH phase with segregated H/N layers and intermixed Ca₂NH phase), suggesting the impact of the phases on the reaction kinetics to be relatively minimal.



1. INTRODUCTION

Ammonia (NH₃) synthesis is a process of fundamental importance to society. It is estimated that billions of people are fed by the fertilizers produced using this process.¹ The synthesis of valuable chemicals (e.g., nitric acid, hydrazine, cyanides, and amino acids) also heavily relies on NH₃. Moreover, NH₃ is an excellent hydrogen carrier for potential fuel applications due to its efficient storage and facile release of H₂.^{2,3} In practice, NH₃ is synthesized by the Haber–Bosch process, which involves harsh operating conditions (400–500 °C, 10–30 MPa) over iron-based catalysts and consumes ~1% of the world's total energy production.⁴ Thus, developing more efficient catalysts for this process is significant. Due to the suitable adsorption energy of N₂ over ruthenium, ruthenium is demonstrated as one of the best single metal catalysts for synthesizing NH₃ under mild conditions.⁵ However, the competitive, strong adsorption of H₂ over the Ru surface is detrimental to the adsorption of N₂. Subsequently, it causes the hydrogen poisoning effect, which exhibits a reaction rate with a negative reaction order of H₂.

It has been reported that using electrides (e.g., C12A7:e⁻ and Ca₂N:e⁻), hydrides (e.g., LnH₂, Ln = La, Ce, or Y), oxyhydrides (e.g., BaTiO_{2.7}H_{0.3}), and calcium amide [Ca(NH₂)₂] as supports for Ru catalysts can suppress the hydrogen poisoning effect by a reversible migration of

hydrogen between Ru and the support.^{6–10} Moreover, the electrides, hydrides, oxyhydrides, and calcium amide-supported Ru catalysts usually show much higher activity than the common alkali-promoted Ru catalysts in NH₃ synthesis. For example, the activation energy over Ru/C12A7:e⁻ (ca. 55 kJ/mol) is only half of that over conventional Ru catalysts due to the promotional effect of C12A7:e⁻ on the dissociation of N₂ on Ru.¹¹ Using Ca₂N:e⁻ as a support for Ru catalysts can significantly improve the performance compared to that of Ru/Ca12A7:e⁻. For example, at 300 °C, the NH₃ synthesis rate is as high as 1674 mmol/(g·h) over 1.8 wt % Ru/Ca₂N:e⁻, while it is only 745 mmol/(g·h) over 1.8 wt % Ru/Ca12A7:e⁻.⁸ For Ru/Ca₂N:e⁻ catalysts, a reaction between the anionic electron of the support and adsorbed hydrogen species produces a hydrogen-deficient Ca₂NH hydride under the NH₃ synthesis condition. H₂ adsorption–desorption experiments and density functional theory (DFT) calculations show that Ca₂NH can be further converted to the Ca₂NH_{1-x} phase with the presence of

Received: December 1, 2022

Revised: February 21, 2023

Ru particles, and $\text{Ca}_2\text{NH}_{1-x}$ has a stronger electron-donation ability than Ca_2NH . $\text{Ca}_2\text{N:e}^-$ has a layered hexagonal structure with layers of $[\text{Ca}_2\text{N}]^+$ separated by anionic electrons.¹² By forming Ca_2NH in the reaction condition, the Ca atoms have a slightly distorted cubic close-packed structure, where N^{3-} and H^- ions are distributed in each anion layer. However, the exact structure derived from $\text{Ca}_2\text{N:e}^-$ under the reaction conditions is still unclear as few characterization tools are available for this aim.

Neutron spectroscopy, i.e., inelastic neutron scattering (INS), is a powerful method to determine the positions and motions of atoms in condensed matter. In particular, the technique is very sensitive to the motion of hydrogen, making it an excellent tool for elucidating the structure of catalysts in hydrogen-involved reactions (e.g., hydrogenation, dehydrogenation, and NH_3 synthesis).¹³ For example, Moon et al. studied the structural change of Ni/BaH₂ in an $\text{N}_2\text{--H}_2$ chemical looping process via the in situ inelastic neutron scattering technique.¹⁴ INS and neutron diffraction results showed that BaH₂ was converted to barium imide (BaNH) in the N_2 reaction step. Using the same methodology, Kammert et al. found that the hydride encaged in the C12A7 electride was stable and not likely to be involved in the ammonia synthesis.¹⁵ Instead, the surface-adsorbed hydrogen was responsible for the reaction's catalytic activity over the Ru/C12A7 electride catalyst. Thus, neutron scattering techniques may provide essential information on the structure of $\text{Ca}_2\text{N:e}^-$ under NH_3 synthesis conditions.

In this work, we first prepared $\text{Ca}_2\text{N:e}^-$ by a solid-state reaction and loaded Ru using the chemical vapor deposition (CVD) method. Then, we applied in situ INS along with first-principles simulations to investigate the evolution of the catalyst structure in NH_3 synthesis. The neutron scattering experiment showed that the Ca_2NH phase likely formed from $\text{Ca}_2\text{N:e}^-$ during NH_3 synthesis and it had a segregated structure with layers of H or N separated by layers of Ca. DFT calculations were performed to study the elementary steps of ammonia synthesis over the obtained segregated Ca_2NH structure. The energetics were compared to those obtained over the regular model of Ca_2NH .

2. EXPERIMENTAL METHODS

2.1. Catalyst Synthesis. $\text{Ca}_2\text{N:e}^-$ was synthesized by a solid-state method using Ca_3N_2 powder and a Ca metal shot. Ca_3N_2 and the Ca metal shot were mixed at a molar ratio of 1:1, and the mixture was pressed into a pellet form under pressure (20–30 MPa). Then, the pellet was covered with molybdenum foil and sealed in an evacuated silica tube. The silica tube was heated at 800 °C for 50 h in vacuum, followed by quenching into water. The obtained sample was then ground into a powder under an Ar atmosphere. Ru-loading on $\text{Ca}_2\text{N:e}^-$ was conducted using a CVD method. The $\text{Ca}_2\text{N:e}^-$ powder and $\text{Ru}_3(\text{CO})_{12}$ were sealed in a stainless-steel container and heated under the following program: using a ramping rate of 2 °C/min for the whole procedure with four temperature steps (increase up to 40 °C and hold for 1 h, increase up to 70 °C and hold for 2 h, increase up to 120 °C and hold for 1 h, and increase up to 250 °C and hold for 2 h). The structure and morphology of Ca_2N were measured by X-ray diffraction (XRD, D/MAX-2500/PC, Rigaku, Japan) analysis with Cu K α radiation ($\lambda = 1.5418$ Å) and scanning electron microscopy (SEM, JSM-7600F, JEOL). The SEM image (Figure S1 in the Supporting Information) and XRD pattern (Figure S2) are similar to those reported in the work by Kitano et al.,⁸ suggesting the successful synthesis of $\text{Ca}_2\text{N:e}^-$. The particle size of Ru on $\text{Ca}_2\text{N:e}^-$ was characterized by both CO chemisorption and high-angle annular dark field (HAADF) scanning transmission electron microscopy (STEM).

The chemisorption result (details in the Supporting Information) and HAADF-STEM image (Figure S3) both showed the Ru particles with a size in the range 2–3 nm.

2.2. Inelastic Neutron Scattering and Neutron Diffraction Measurement. In situ INS experiment was conducted at the VISION beamline (BL-16B) of Spallation Neutron Source, Oak Ridge National Laboratory. 1.7 g of the Ru/ $\text{Ca}_2\text{N:e}^-$ sample was loaded into a stainless-steel can with a stop valve at one end in a glovebox for the experiment. The sample was evacuated at room temperature and cooled down to -268.15 °C to obtain a fresh sample INS background spectrum. Then, the sample was heated up to 350 °C in vacuum, and a mixture of H_2 and N_2 with a molar ratio (H_2/N_2) of 3 at 1 bar was introduced into the cell at the same temperature and held for 3 h. After that, the cell was cooled down to RT and vacuumed. After the reaction, the INS measurement of the catalyst was conducted at -268.15 °C (spectrum name: Ru/ $\text{Ca}_2\text{N--H}_2/\text{N}_2$). Then, the catalyst was treated with H_2 and N_2 to examine the phase change. For H_2 treatment, the cell temperature was elevated back to 350 °C, followed by allowing H_2 to flow in the cell for 3 h at 1 bar. Then, the cell was cooled down to RT and vacuumed. The INS measurement of the H_2 -treated catalyst was conducted at -268.15 °C (spectrum name: Ru/ $\text{Ca}_2\text{N--H}_2$ -1st). For N_2 treatment, the cell temperature was elevated back to 350 °C, followed by filling N_2 into the cell for 3 h before evacuation at RT and spectral collection at -268.15 °C (spectrum name: Ru/ $\text{Ca}_2\text{N--N}_2$ -1st). The H_2 treatment and neutron scattering measurement were repeated one more time (spectrum name: Ru/ $\text{Ca}_2\text{N--H}_2$ -2nd). Then, the cell was heated at 350 °C, and N_2 was introduced into the cell with 1 bar for 25 min and then vacuumed shortly to refill the N_2 with 1 bar. This vacuum and N_2 filling cycle was repeated 3 times. The cell was cooled down to RT followed by vacuum. The INS spectrum of the sample was obtained at -268.15 °C (spectrum name: Ru/ $\text{Ca}_2\text{N--N}_2$ -2nd). To evaluate the change of structure over the temperature (600 °C) where the formed nitrogen and hydrogen can be removed, the cell was continuously evacuated to vacuum at 350 and 600 °C, and INS spectra were obtained at -268.15 °C (spectra name: Ru/ $\text{Ca}_2\text{N--vacuum-350}$ °C, Ru/ $\text{Ca}_2\text{N--vacuum-600}$ °C, respectively).

2.3. DFT Calculations. DFT calculations were performed using the Vienna Ab Initio Simulation Package (VASP).^{16,17} The projector-augmented wave method was used to describe the electron–core interaction, and a kinetic energy cutoff of 450 eV was used.¹⁸ The Perdew–Burke–Ernzerhof functional form of generalized-gradient approximation was used for electron exchange and correlation energies.¹⁹ All calculations were performed, including spin polarization. A $2 \times 2 \times 1$ sampling of the Brillouin zone using a Monkhorst–Pack scheme was used for the k-points.²⁰ Dispersion corrections were added using the method by Grimme.²¹ A vacuum layer of 15 Å was used for the surface slabs. Transition states were found with the nudged elastic band and the dimer method implemented in the VASP–VTST package with a force convergence criterion of 0.05 eV/Å.^{22,23}

3. RESULTS AND DISCUSSION

3.1. In Situ INS Study. Although Ru/ $\text{Ca}_2\text{N:e}^-$ demonstrates excellent ammonia synthesis performance at ambient pressure, the structural evolution of the $\text{Ca}_2\text{N:e}^-$ electride lacks direct spectroscopic evidence.⁸ Here, we employed INS to follow the structural changes of Ru/ $\text{Ca}_2\text{N:e}^-$ under different conditions, including simulated ammonia synthesis and cycling conditions. The results are shown in Figure 1. After the initial reaction, additional neutron scattering intensities at 562, 711, and 762 cm^{-1} (Figure 1a) suggested that hydrogen-containing species were formed in the sample, most likely Ca_2NH via the reaction of the electride with hydrogen.⁸ After the first H_2 reaction (Figure 1b), the intensity of most peaks became stronger, while the profile of the spectrum remained largely the same, indicating that more of the same H-containing species had formed. After the first N_2 reaction (Figure 1c), there was a

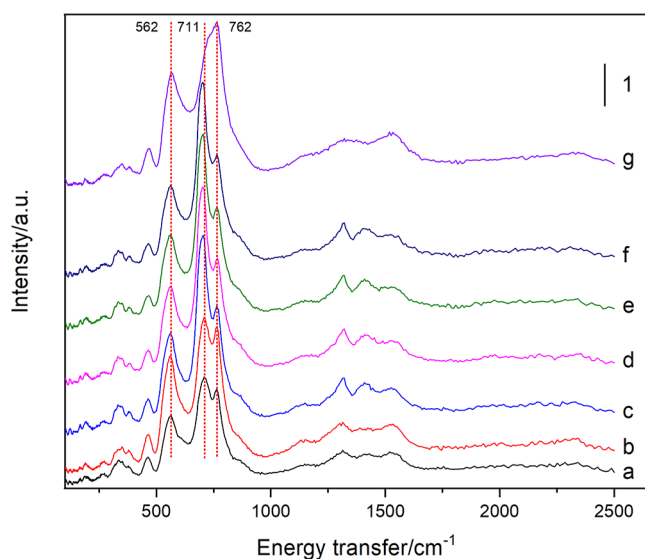


Figure 1. INS spectra of the sample in different treatments. (a) Ru/Ca₂N–H₂/N₂, (b) Ru/Ca₂N–H₂-1st, (c) Ru/Ca₂N–N₂-1st, (d) Ru/Ca₂N–H₂-2nd, (e) Ru/Ca₂N–N₂-2nd, (f) Ru/Ca₂N–vacuum-350 °C, and (g) Ru/Ca₂N–vacuum-600 °C. All the spectra were obtained by subtracting the obtained spectrum from the background spectrum of a fresh Ru/Ca₂N:e[−].

noticeable change in the peak profile. Specifically, the intensity of the peaks at ~ 550 and ~ 760 cm^{−1} decreased, while that of the peak at ~ 710 cm^{−1} increased. These differences suggested that the environment of hydrogen in the catalyst structure had changed, possibly due to the formation of a new phase(s). The subsequent H₂ and N₂ reactions and the 350 °C vacuum did not lead to further changes in the spectral features (Figure 1d–f), indicating the relatively stable structure of the newly formed phase under these conditions. However, an evacuation at 600 °C reduced the peak intensity at 711 cm^{−1} significantly (Figure 1g), accompanied by an increase of intensity at lower (i.e., ~ 562 cm^{−1}) and higher (i.e., ~ 762 cm^{−1}) frequencies. The total scattered intensity, which scaled with the total amount of hydrogen, did not change significantly, suggesting a more likely restructuring of the catalyst than the loss of H-containing species during the high-temperature vacuum treatment.

To understand these observations, simulated INS spectra were obtained based on various structural models of Ca₂NH (Figure 2). The Ca₂N (PDF: 70-4196) and Ca₂NH (PDF: 76-608) have a space group $R\bar{3}m$ and $Fd\bar{3}m$, respectively. First, phonon calculations (lattice dynamics) were performed on Ca₂NH using the structure reported in the literature (Figure 2d).⁸ The simulated VISION spectrum on this model (red, labeled as “Ca₂NH bulk model” in Figure 2a) bore some similarities with the measured one, but there were also apparent differences.²⁴ Most notably, the peak at ~ 400 cm^{−1} in the simulation, presumably corresponding to the peak at 550 cm^{−1} in the experiment, was significantly underestimated in frequency and was much sharper than the one observed in the experiment. We then adopted a different structure model for Ca₂NH, in which instead of having mixed N and H between the Ca layers, N and H were segregated (Figure 2e). The simulated VISION spectrum on this model is shown as the blue spectrum in Figure 2a, labeled as the “Ca₂NH segregated model”. This structure was closer to the original Ca₂N structure (Figure 2c) and could be obtained easily by “inserting” the hydrogen layers into the Ca₂N:e[−] structure.

Phonon calculation of this structure produced a VISION spectrum (blue in Figure 2a) much closer to that observed in the experiment, but the peak positions still had a systematic red shift. Finally, the effects of phonon anharmonicity were examined by running a molecular dynamics (MD) simulation and converting the MD trajectory into the simulated spectrum.²⁵ Since the MD simulation overcomes the limitations of harmonic approximation in the phonon calculation, it does consider the anharmonicity of the local potential energy profile. Indeed, the MD-directed VISION spectrum from the Ca₂NH segregated model was even more similar to the experiment, showing excellent agreement in all major peak positions (Figure 2b). Thus, according to the neutron scattering data, we hypothesized that the H and N atoms were located in different layers separated by the Ca layer, i.e., a segregated structure (Figure 2e), drastically different from the traditional mixed structure, as shown in Figure 2d.

Other models of Ca₂NH [completely random/uncorrelated distribution of N and H, and ordered distribution ($Fd\bar{3}m$) with a N/H ratio of 3/1 in one layer and 1/3 in the alternate layer] have also been tested, and the corresponding simulated INS spectra are compared with the experimental spectrum (Figure S4). However, the results indicated that these two models both exhibited significant discrepancies to the experimentally observed spectrum. Although our modeling did not (and could not) consider all possible N/H distribution scenarios, the available results suggested that the real structure of Ca₂NH must have a high degree of N/H segregation.

The above comparison confirmed the Ca₂NH phase structure after the initial and first H₂ reactions. The first N₂ reaction led to a rather sharp peak near 710 cm^{−1}. We speculated that it was due to the insertion of N into Ca₂NH, leading to a partial transition toward CaNH. To this end, the INS spectrum of CaNH was simulated. As shown in Figure 3, compared to Ca₂NH, where two distinct peaks were observed at lower (500–600 cm^{−1}) and higher (700–800 cm^{−1}) frequencies, in CaNH, the INS intensities were concentrated at ~ 800 cm^{−1}, with no apparent intensities at frequencies lower than 700 cm^{−1}. This was qualitatively consistent with the observed changes upon N₂ reaction. The evacuation at 600 °C likely removed some of the N from the system, partially reversing the reaction. In this case, we noted that the simulation of CaNH did not fully explain the experimental observation, possibly because only a fraction of Ca₂NH was transformed into the CaNH phase under the experiment condition, e.g., a mixture of Ca₂NH and CaNH in the sample.

3.2. DFT Study. Since our INS results suggested an unusual working structure for Ca₂NH in Ru/Ca₂N:e[−] under simulated ammonia synthesis conditions, we were motivated to understand if there were any catalytic implications on the reaction mechanisms of ammonia synthesis. This was approached by DFT in exploring the mechanism of ammonia synthesis on Ru/Ca₂NH with two different Ca₂NH structures: the regular one and the segregated one (Figure 2).

We started to perform our mechanistic studies on a model containing the normal Ca₂NH phase, exposing the same (111) facet as the Ca₂N phase. The structure models for the as-synthesized Ru/Ca₂N and Ru/Ca₂NH normal phases are shown in Figure S5. The model contained a supported Ru₁₉ nanoparticle with a diameter of 0.8 nm, close to previous experimental observations and within computational feasibility.²⁶ Using the free energy of formation as a stability metric,

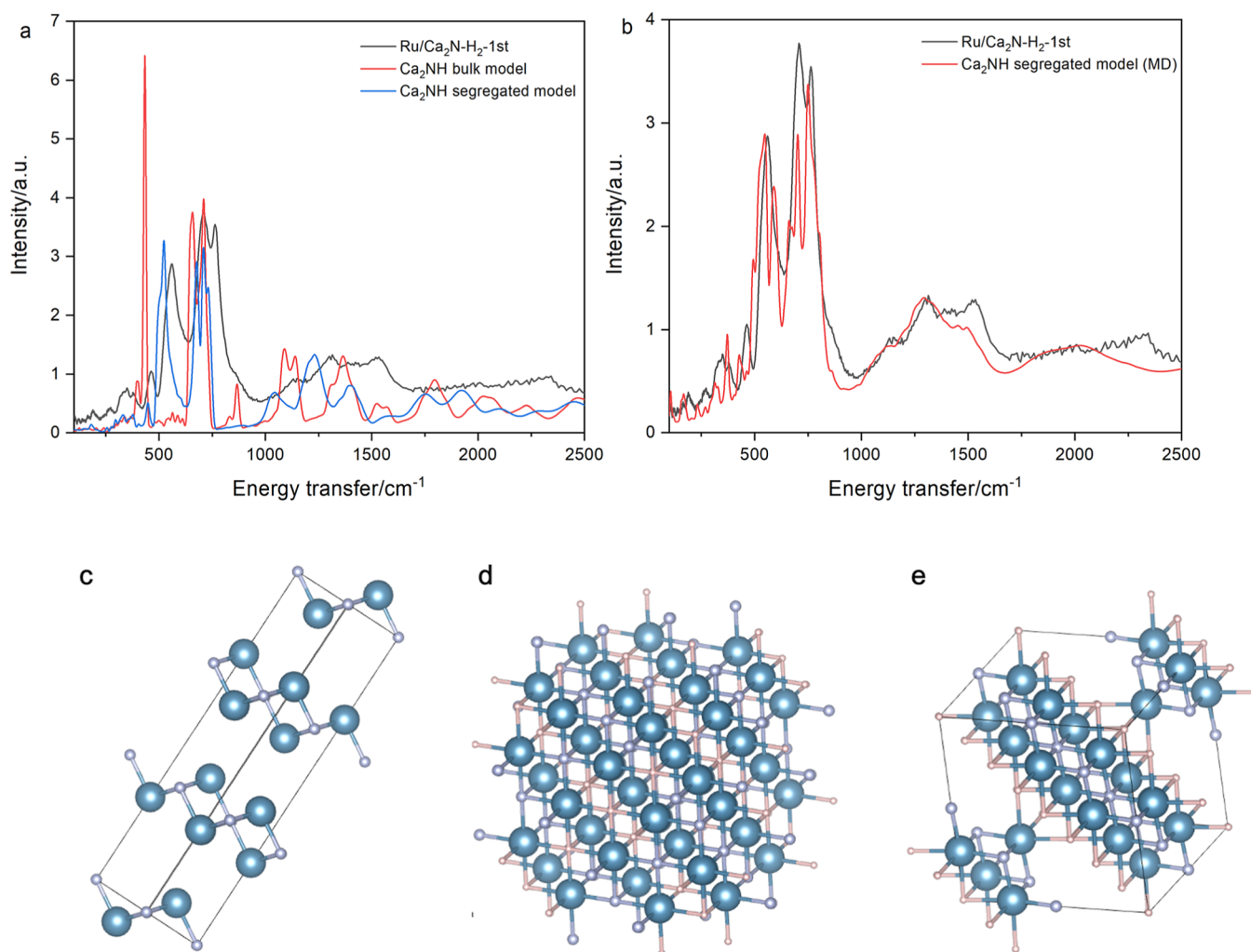


Figure 2. (a,b) INS spectra of Ru/Ca₂N in H₂ at 350 °C in the first cycle (black) and the comparison with simulated spectra from different models (blue and red). (c) Structure of the original Ca₂N. (d) Literature structure model of Ca₂NH showing mixed N and H distribution, corresponding to the red spectrum in (a). (e) The H/N segregated model proposed in this work is closer to the original Ca₂N in (c). It can be obtained by inserting a H layer between the original Ca₂N layers. The simulated INS spectra from this model are shown in blue in (a) (using lattice dynamics based on harmonic approximation) and red in (b) (using molecular dynamics to include anharmonicity).

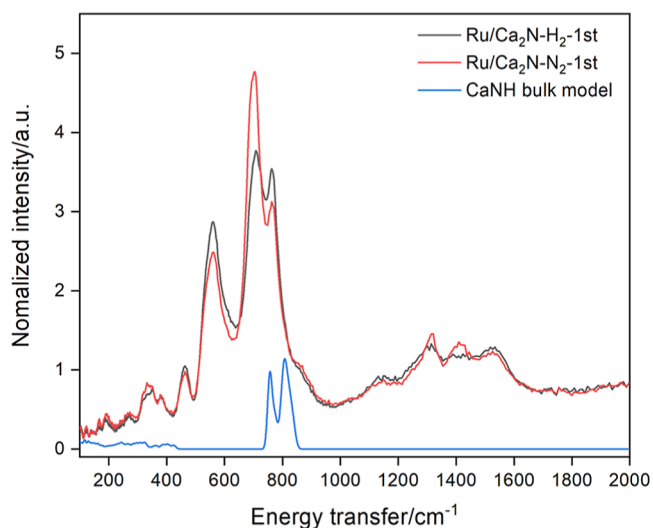


Figure 3. INS spectra of Ru/Ca₂N in H₂ and N₂ at 350 °C in the first cycle and the comparison with the CaNH bulk model.

we found that under the reaction conditions, the Ca₂NH phase had a lower free energy than that of pure Ru/Ca₂N and was consistent with experimental observations (Figure S6). Meanwhile, additional nitrogen could be found occupying the interfacial regions of the Ru and Ca₂N surfaces. This picture was consistent with a strong Ru–surface interaction aided by surface N as proposed by Hosono et al.²⁶ We, therefore, used a Ru/Ca₂NH with interfacial “lattice” N as a starting point in our calculations of the ammonia synthesis mechanism.

We began by investigating the H₂ dissociation process on an initially bare Ru nanoparticle supported on Ca₂NH. We found that the dissociation at the edges was nearly spontaneous upon adsorption and exothermic, with a reaction energy of -1.26 eV. Hence it was safe to assume that the H coverage on Ru was both kinetically and thermodynamically favorable, leading to the well-established H-poisoning phenomenon which occurs in ammonia synthesis. This was also confirmed by DFT calculations showing a hydrogen-covered nanoparticle to be the most stable state under reaction conditions (Figure S6). Given the blocking of the potential active sites by hydrogen, it is unlikely for nitrogen dissociation and hydrogenation to occur on the surface of the particle itself, which already has a

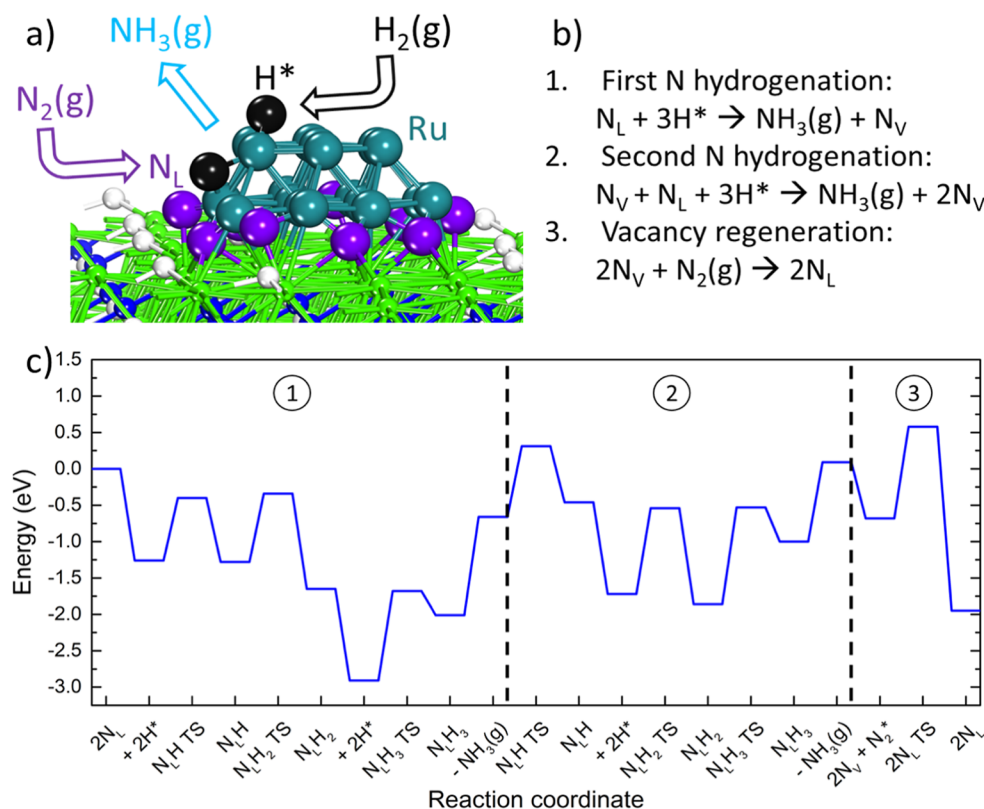


Figure 4. (a) Illustration of the ammonia synthesis mechanism involving the interfacial lattice nitrogen and hydrogen adsorbed on the nanoparticle H^* . (b) Breakdown of the ammonia synthesis mechanism involving successive nitrogen hydrogenation steps followed by a vacancy regeneration step with N_2 . (c) Energy profile of the overall reaction $N_2 + 3H_2 \rightarrow 2NH_3$.

high barrier of 1.28 eV on the bare surface. Instead, we hypothesized that nitrogen hydrogenation could first occur at the interfacial N sites, as previously noted, proceeding via a Mars–van Krevelen (MVK) mechanism (Figure 4a). Figure 4c shows the energy profile from DFT calculations for the reaction $N_2 + 3H_2 \rightarrow 2NH_3$. Two successive hydrogenation steps on lattice nitrogen (N_L) were mapped out, leaving two nitrogen vacancies, which were then filled by N_2 from the gas phase (Figure 4b). We found that the rate-limiting step was likely the step from NH_2 to NH_3 , which had a high barrier for both the first and second nitrogen hydrogenation steps. Alternatively, we considered a branching mechanism where N_2 reacted with a single vacancy rather than a divacancy, and hydrogenation occurred on the non-bound N in the adsorbed N_2 (Figure S7). We noted that both pathways were viable with similar rate-limiting elementary steps, and in both cases, nitrogen hydrogenation occurred at the interfacial sites rather than on the Ru nanoparticle. As we found that nitrogen was more stably bound on the interface and hydrogen more stably bound on the particle, competition between the two reactants was entirely avoided.

Subsequently, since neutron studies revealed a new segregated Ca_2NH phase with alternating layers of H and N, we recalculated the energy profile for the first N hydrogenation step. We compared the energetics with the mixed Ca_2NH phase (Figure S8). We found minor changes in the barriers and thermodynamics between the two phases, suggesting the impact of the phase on the calculation results to be minimal. We also studied the kinetics and thermodynamics of hydrogen diffusion from the subsurface to the surface to participate in the hydrogenation reaction (Figure S9). While surface to

subsurface migration could be facile, the migration from the subsurface to the surface was kinetically and thermodynamically unfavorable. The hydrogenation of lattice N by surface hydrogen was also found to have a higher barrier, 1.40 eV, compared to that of hydrogen on Ru, with a barrier of 0.86 eV. As a consequence, the contribution of subsurface hydrogen to ammonia synthesis on this catalyst could be considered to be minimal.

4. CONCLUSIONS

In this work, the structural change of a $Ru/Ca_2N:e^-$ catalyst in NH_3 synthesis was studied by in situ INS, and its catalytic implication was revealed via DFT modeling. During NH_3 synthesis, both INS and DFT results show that the $Ca_2N:e^-$ phase is likely converted to Ca_2NH by reacting with hydrogen species. A segregated Ca_2NH model calculated by molecular dynamics could well replicate the majority spectral features of those observed in the in situ INS study, indicating that the H and N atoms of the Ca_2NH phase are located in different layers separated by the Ca layer, different from the normal phase with N and H mixed in the same layer. DFT calculations of ammonia synthesis pathways suggest that additional nitrogen atoms occupy the interfacial regions of the Ru and Ca_2N surfaces. Nitrogen hydrogenation proceeds via a MVK mechanism at the interfacial N sites. However, differences in the two different phases (Ca_2NH with segregated H/N layers and mixed Ca_2NH phase) minimally influence the barriers and thermodynamics of the first N hydrogenation step. Moreover, hydrogen migration from the subsurface to the surface is kinetically and thermodynamically unfavorable, which may rule

out the participation of sub-surface hydrogen of Ca₂NH in the reaction.

Even though the impact on the reaction mechanisms of the segregated Ca₂NH structure seems minimal from DFT compared to the regular mixed phase, it is still worthwhile to draw attention from this research field to this unusual structure that may provide insights into some experimental observations. It remains an interesting task to prepare the two different Ca₂NH phases as supports for Ru and study their performances experimentally in ammonia synthesis.

■ ASSOCIATED CONTENT

SI Supporting Information

The Supporting Information is available free of charge at <https://pubs.acs.org/doi/10.1021/acs.chemmater.2c03599>.

Detailed experimental results on XRD, SEM, CO chemisorption, and HAADF-STEM and additional modeling and DFT results (PDF)

■ AUTHOR INFORMATION

Corresponding Authors

Victor Fung – Center for Nanophase Materials Sciences (CNMS), Oak Ridge National Laboratory, Oak Ridge, Tennessee 37831, United States; orcid.org/0000-0002-3347-6983; Email: victorfung88@hotmail.com

Zili Wu – Chemical Sciences Division, Oak Ridge National Laboratory, Oak Ridge, Tennessee 37831, United States; Center for Nanophase Materials Sciences (CNMS), Oak Ridge National Laboratory, Oak Ridge, Tennessee 37831, United States; orcid.org/0000-0002-4468-3240; Email: wuz1@ornl.gov

Authors

Xinbin Yu – Chemical Sciences Division, Oak Ridge National Laboratory, Oak Ridge, Tennessee 37831, United States; Center for Nanophase Materials Sciences (CNMS), Oak Ridge National Laboratory, Oak Ridge, Tennessee 37831, United States

Jisue Moon – Chemical Sciences Division, Oak Ridge National Laboratory, Oak Ridge, Tennessee 37831, United States; Center for Nanophase Materials Sciences (CNMS), Oak Ridge National Laboratory, Oak Ridge, Tennessee 37831, United States

Yongqiang Cheng – Neutron Science Directorate, Oak Ridge National Laboratory, Oak Ridge, Tennessee 37831, United States; orcid.org/0000-0002-3263-4812

Luke Daemen – Neutron Science Directorate, Oak Ridge National Laboratory, Oak Ridge, Tennessee 37831, United States

Jue Liu – Neutron Science Directorate, Oak Ridge National Laboratory, Oak Ridge, Tennessee 37831, United States; orcid.org/0000-0002-4453-910X

Sung Wng Kim – Department of Energy Science, Sungkyunkwan University, Suwon 16419, Republic of Korea; orcid.org/0000-0002-4802-5421

Abinash Kumar – Center for Nanophase Materials Sciences (CNMS), Oak Ridge National Laboratory, Oak Ridge, Tennessee 37831, United States

Miaofang Chi – Center for Nanophase Materials Sciences (CNMS), Oak Ridge National Laboratory, Oak Ridge, Tennessee 37831, United States; orcid.org/0000-0003-0764-1567

Anibal J. Ramirez-Cuesta – Neutron Science Directorate, Oak Ridge National Laboratory, Oak Ridge, Tennessee 37831, United States

Complete contact information is available at:

<https://pubs.acs.org/doi/10.1021/acs.chemmater.2c03599>

Author Contributions

[†]X.Y. and J.M. contributed equally to this work.

Notes

The authors declare no competing financial interest.

This manuscript has been authored in part by UT-Battelle, LLC, under contract DE-AC05-00OR22725 with the US Department of Energy (DOE). The US government retains and the publisher, by accepting the article for publication, acknowledges that the US government retains a nonexclusive, paid-up, irrevocable, worldwide license to publish or reproduce the published form of this manuscript, or allow others to do so, for US government purposes. DOE will provide public access to these results of federally sponsored research in accordance with the DOE Public Access Plan (<http://energy.gov/downloads/doe-public-access-plan>).

■ ACKNOWLEDGMENTS

This research was sponsored by the Laboratory Directed Research Development (LDRD) of Oak Ridge National Laboratory, managed by UT-Battelle, LLC, for the U.S. Department of Energy. X.Y., M.C., and Z.W. were partly supported by the U.S. Department of Energy, Office of Science, Office of Basic Energy Sciences, Chemical Sciences, Geosciences, and Biosciences Division, Catalysis Science program. The computing resources were made available through the VirtuES and the ICE-MAN projects, funded by Laboratory Directed Research and Development program and Compute and Data Environment for Science (CADES) at ORNL. The neutron studies were conducted at the Spallation Neutron Source, a DOE Office of Science User Facility operated by the Oak Ridge National Laboratory. Part of the work including the sample preparation and electron microscopy was conducted as a part of a user project at the Center for Nanophase Materials Sciences, which is a US Department of Energy, Office of Science User Facility at Oak Ridge National Laboratory.

■ REFERENCES

- (1) Erisman, J. W.; Sutton, M. A.; Galloway, J.; Klimont, Z.; Winiwarter, W. How a century of ammonia synthesis changed the world. *Nat. Geosci.* **2008**, *1*, 636–639.
- (2) Satyapal, S.; Petrovic, J.; Read, C.; Thomas, G.; Ordaz, G. The U.S. Department of Energy's National Hydrogen Storage Project: Progress towards meeting hydrogen-powered vehicle requirements. *Catal. Today* **2007**, *120*, 246–256.
- (3) Makepeace, J. W.; He, T.; Weidenthaler, C.; Jensen, T. R.; Chang, F.; Vegge, T.; Ngene, P.; Kojima, Y.; de Jongh, P. E.; Chen, P.; David, W. I. F. Reversible ammonia-based and liquid organic hydrogen carriers for high-density hydrogen storage: Recent progress. *Int. J. Hydrogen Energy* **2019**, *44*, 7746–7767.
- (4) Capdevila-Cortada, M. Electrifying the Haber-Bosch. *Nat. Catal.* **2019**, *2*, 1055.
- (5) Karim, A. M.; Prasad, V.; Mpourmpakis, G.; Lonergan, W. W.; Frenkel, A. I.; Chen, J. G.; Vlachos, D. G. Correlating Particle Size and Shape of Supported Ru/ γ -Al₂O₃ Catalysts with NH₃ Decomposition Activity. *J. Am. Chem. Soc.* **2009**, *131*, 12230–12239.

- (6) Nakao, T.; Tada, T.; Hosono, H. First-principles and microkinetic study on the mechanism for ammonia synthesis using Ru-loaded hydride catalyst. *J. Phys. Chem. C* **2019**, *124*, 2070–2078.
- (7) Kitano, M.; Inoue, Y.; Yamazaki, Y.; Hayashi, F.; Kanbara, S.; Matsuishi, S.; Yokoyama, T.; Kim, S. W.; Hara, M.; Hosono, H. Ammonia synthesis using a stable electride as an electron donor and reversible hydrogen store. *Nat. Chem.* **2012**, *4*, 934–940.
- (8) Kitano, M.; Inoue, Y.; Ishikawa, H.; Yamagata, K.; Nakao, T.; Tada, T.; Matsuishi, S.; Yokoyama, T.; Hara, M.; Hosono, H. Essential role of hydride ion in ruthenium-based ammonia synthesis catalysts. *Chem. Sci.* **2016**, *7*, 4036–4043.
- (9) Tang, Y.; Kobayashi, Y.; Masuda, N.; Uchida, Y.; Okamoto, H.; Kageyama, T.; Hosokawa, S.; Loyer, F.; Mitsuhara, K.; Yamanaka, K.; Tamenori, Y.; Tassel, C.; Yamamoto, T.; Tanaka, T.; Kageyama, H. Metal-Dependent Support Effects of Oxyhydride-Supported Ru, Fe, Co Catalysts for Ammonia Synthesis. *Adv. Energy Mater.* **2018**, *8*, 1801772.
- (10) Inoue, Y.; Kitano, M.; Kishida, K.; Abe, H.; Niwa, Y.; Sasase, M.; Fujita, Y.; Ishikawa, H.; Yokoyama, T.; Hara, M.; Hosono, H. Efficient and stable ammonia synthesis by self-organized flat Ru nanoparticles on calcium amide. *ACS Catal.* **2016**, *6*, 7577–7584.
- (11) Kitano, M.; Kanbara, S.; Inoue, Y.; Kuganathan, N.; Sushko, P. V.; Yokoyama, T.; Hara, M.; Hosono, H. Electride support boosts nitrogen dissociation over ruthenium catalyst and shifts the bottleneck in ammonia synthesis. *Nat. Commun.* **2015**, *6*, 6731–9.
- (12) Lee, K.; Kim, S. W.; Toda, Y.; Matsuishi, S.; Hosono, H. Dicalcium nitride as a two-dimensional electride with an anionic electron layer. *Nature* **2013**, *494*, 336–340.
- (13) Wu, Z.; Cheng, Y.; Tao, F.; Daemen, L.; Foo, G. S.; Nguyen, L.; Zhang, X.; Beste, A.; Ramirez-Cuesta, A. J. Direct neutron spectroscopy observation of cerium hydride species on a cerium oxide catalyst. *J. Am. Chem. Soc.* **2017**, *139*, 9721–9727.
- (14) Moon, J.; Cheng, Y.; Daemen, L.; Novak, E.; Ramirez-Cuesta, A. J.; Wu, Z. On the structural transformation of Ni/BaH₂ during a N₂-H₂ chemical looping process for ammonia synthesis: a joint in situ inelastic neutron scattering and first-principles simulation study. *Top. Catal.* **2021**, *64*, 685–692.
- (15) Kammert, J.; Moon, J.; Cheng, Y.; Daemen, L.; Irlle, S.; Fung, V.; Liu, J.; Page, K.; Ma, X.; Phaneuf, V.; Tong, J.; Ramirez-Cuesta, A. J.; Wu, Z. Nature of reactive hydrogen for ammonia synthesis over a Ru/C12A7 electride catalyst. *J. Am. Chem. Soc.* **2020**, *142*, 7655–7667.
- (16) Kresse, G.; Furthmüller, J. Efficiency of ab-initio total energy calculations for metals and semiconductors using a plane-wave basis set. *Comput. Mater. Sci.* **1996**, *6*, 15–50.
- (17) Kresse, G.; Furthmüller, J. Efficient iterative schemes for ab initio total-energy calculations using a plane-wave basis set. *Phys. Rev. B: Condens. Matter Mater. Phys.* **1996**, *54*, 11169.
- (18) Blöchl, P. E. Projector augmented-wave method. *Phys. Rev. B: Condens. Matter Mater. Phys.* **1994**, *50*, 17953.
- (19) Perdew, J. P.; Burke, K.; Ernzerhof, M. Generalized gradient approximation made simple. *Phys. Rev. Lett.* **1996**, *77*, 3865.
- (20) Monkhorst, H. J.; Pack, J. D. Special points for Brillouin-zone integrations. *Phys. Rev. B: Condens. Matter Mater. Phys.* **1976**, *13*, 5188.
- (21) Grimme, S.; Antony, J.; Ehrlich, S.; Krieg, H. A consistent and accurate ab initio parametrization of density functional dispersion correction (DFT-D) for the 94 elements H-Pu. *J. Chem. Phys.* **2010**, *132*, 154104.
- (22) Henkelman, G.; Uberuaga, B. P.; Jónsson, H. A climbing image nudged elastic band method for finding saddle points and minimum energy paths. *J. Chem. Phys.* **2000**, *113*, 9901–9904.
- (23) Henkelman, G.; Jónsson, H. A dimer method for finding saddle points on high dimensional potential surfaces using only first derivatives. *J. Chem. Phys.* **1999**, *111*, 7010–7022.
- (24) Cheng, Y.; Daemen, L. L.; Kolesnikov, A. I.; Ramirez-Cuesta, A. J. Simulation of inelastic neutron scattering spectra using OCLIMAX. *J. Chem. Theory Comput.* **2019**, *15*, 1974–1982.
- (25) Cheng, Y.; Kolesnikov, A. I.; Ramirez-Cuesta, A. J. Simulation of inelastic neutron scattering spectra directly from molecular dynamics trajectories. *J. Chem. Theory Comput.* **2020**, *16*, 7702–7708.
- (26) Abe, H.; Niwa, Y.; Kitano, M.; Inoue, Y.; Sasase, M.; Nakao, T.; Tada, T.; Yokoyama, T.; Hara, M.; Hosono, H. Anchoring Bond between Ru and N Atoms of Ru/Ca2NH Catalyst: Crucial for the High Ammonia Synthesis Activity. *J. Phys. Chem. C* **2017**, *121*, 20900–20904.